

Research Article

TiO₂ Films for Self-Detection and Decontamination

Laura R. Skubal,¹ Alan L. McArthur,¹ and Matthew Newville²

¹ Chemical Sciences Division, Argonne National Laboratory, 9700 South Cass Avenue, Argonne, IL 60439, USA

² Consortium for Advanced Radiation Science, The University of Chicago, 9700 South Cass Avenue, Argonne, IL 60439, USA

Correspondence should be addressed to Laura R. Skubal, l@anl.gov

Received 25 July 2007; Accepted 05 March 2008

Recommended by Russell Howe

Methods that rapidly detect, characterize, quantify, and decontaminate surfaces are essential following chemical or biological incidents. Our work focused on developing a “smart” surface, one that monitors itself and the overlying atmosphere and triggers a decontamination step when surface contamination is detected. Titanium dioxide was used to coat a ceramic surface containing skeletal impregnated platinum electrodes. The electrical resistance of the surface became altered by the introduction of a contaminant into the overlying atmosphere and its chemisorption to the surface. This change in resistance in turn initiated illumination by an external ultraviolet lamp to induce photocatalytic oxidation of the sorbed contaminant. Film resistance was concentration-dependent, allowing self-decontamination to be triggered at set pollutant levels. Preliminary results suggest that advanced surfaces and films can be developed to identify contaminant type and concentration and to initiate photocatalytic decontamination to meet regulatory or safety standards.

Copyright © 2008 Laura R. Skubal et al. This is an open access article distributed under the Creative Commons Attribution License, which permits unrestricted use, distribution, and reproduction in any medium, provided the original work is properly cited.

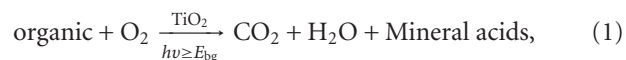
1. INTRODUCTION

Recent advancements in materials have prompted researchers to investigate new ways of combating chemical and biological incidents and contamination. The development and use of self-cleaning materials are prevalent. Numerous studies have been performed that detail the creation, effectiveness, and benefit of self-cleaning films and materials. These studies are especially prevalent for fabrics, glass, and building materials. These studies, however, are only precursors to “smart” materials of the future; materials that incorporate multifunctional particles that will have the ability to detect toxics on their surfaces, identify the toxic, decontaminate themselves, and know when to stop self-decontamination processes. The research presented in this study is a rudimentary approach to creating a material that fulfills these criteria.

In the 1990s, the number of articles describing the benefits of semiconductor photocatalysis for mineralizing organics and reducing metals increased exponentially as compared to the number of articles published before this era. Studies demonstrated that semiconductor photocatalysis was able to effectively decompose a huge variety of organic compounds on particle surfaces, despite the fact that these

organics had structures and functional groups that were vastly different from each other. Alkanes, ketones, alcohols, phenols, aromatic compounds, and so forth all can be mineralized by photocatalysis with titanium dioxide [1–4]. The vast number of decomposition reactions attainable with TiO₂ has led to the incorporation of these particles in materials designed for practical applications.

One of the fastest growing areas of TiO₂ application is the incorporation of reactive particles in surface materials. As Mills and Wang eloquently note the reaction



where E_{bg} , the TiO₂ semiconductor bandgap (3.0 to 3.2 eV), has been used extensively to create self-cleaning surfaces, including glasses, tiles, and fabrics, and has led to the commercialization of these products and a booming industry for them [5]. Their own work reported on the effectiveness of using self-cleaning films composed of Degussa P25 TiO₂-coated quartz discs for the destruction of stearic acid [5]. Other researchers have studied a variety of coatings for decontamination purposes as well. Allen et al. reported on the longevity and effectiveness of anatase and rutile TiO₂ in

paints for self-cleansing and microbial destruction [6], and Abdullah et al. reported on the advantages and disadvantages of coating methods (dip coating, splatter coating, static brush coating, etc.) for various TiO_2 for self-cleaning applications [7]. Other popular applications include the incorporation of photocatalytic semiconductor particles in textiles. Bozzi et al. tried to increase the ability to bond TiO_2 to wool-polyamide and polyester fabrics to improve stain mineralization with some success [8]. Similarly, Qi et al. coated cotton textiles with TiO_2 to create a fabric to reduce bacterial activity and get rid of stains [9]. Research focusing on self-cleaning entities is in its infancy; as the characteristics of nanoparticles are better understood, advancements will be made in these applications.

One aspect of self-cleaning films that has not been well explored includes films that report when they are contaminated, identify the contaminant and concentration of the contaminant, initiate a mechanism to “self-clean,” assess themselves as to when the film surface is restored, and stop the self-cleaning process. This group’s previous work demonstrated that TiO_2 films could be used to detect and distinguish various compounds [10, 11]. The work presented in this paper describes the creation of a film that self-senses contaminants sorbed to it, identifies the concentration of the contaminant, and triggers a mechanism to clean itself.

2. EXPERIMENTAL

2.1. Film preparation

The support substrate for the films was created by depositing fine platinum electrodes on thin aluminum oxide substrates. The aluminum oxide substrates (Coors Corporation, Colo, USA) were screened with platinum electrodes using a conductor paste (Heraeus, Hanau, Germany conductor paste product LP11-4493) silk-screened using a Presco Model 873 screen printer outfitted with Ikegami optics. The electrodes were air-dried, then sintered in a Lindberg type 51524 furnace. The temperature was initially ramped to 350°C over two hours to remove the organic vehicle (Heraeus vehicle RV-025), in which the platinum particles were suspended. The temperature was then increased to 1300°C to sinter the platinum particles. Substrates containing the impregnated platinum electrodes were cooled to ambient temperatures. Degussa P25 TiO_2 was mixed with the organic vehicle in a ratio of 1.0g TiO_2 to 6.5g organic vehicle. The TiO_2 paste was screen printed on top of the platinum electrodes. Substrates housing the electrodes and TiO_2 were fired at 350°C to remove the organic vehicle. Studies in the literature show that a change in Degussa P25 TiO_2 photoreactivity does not accompany firing at this temperature [12].

2.2. Feedback system

The electrodes on finished coated substrates were connected to a system that included an ultraviolet (UV) light emitting diode (LED) (Part BP200CUV1K-250) (Ledtronics, Inc., Calif, USA,) powered by a BK Precision DC Power Supply 1635A. Electrode leads initially were connected to a Wavetek

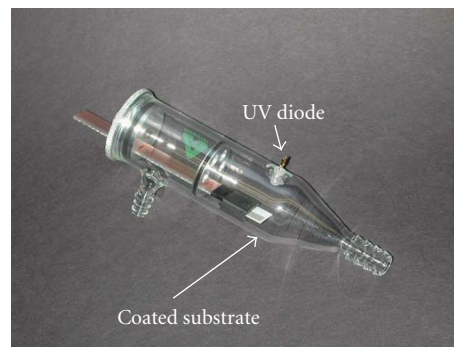


FIGURE 1: 100 mL reactor with two access ports, UV diode, and electrode-connected substrate holder.

DM23XT multimeter to get baseline resistance readings that determined cutoff resistance points. Afterwards, the electrodes of the sensor were connected to the input of an electronic switching circuit that activated the UV LED. The coated substrates and UV diode were contained inside of a sealed quartz chamber. The system configuration is shown in Figure 1.

2.3. Ethanol preparation

Reactor access ports, containing septa, were used to inject various concentrations of ethanol (Aaper Alcohol & Chemical Company, Ky, USA, absolute, 200 proof) into the reactor. Stock gaseous ethanol was prepared by injecting 5 mL of ethanol into a sealed glass bottle with a septum. The ethanol was allowed to equilibrate so that the headspace was saturated (approximately 59000 ppmv). Specific aliquots of ethanol vapor in the headspace were withdrawn via a gas-tight syringe and injected into the reactor to produce specific concentrations of ethanol in the reactor. Dry zero chromatographic air (AGA) periodically was injected into the reactor to replace the air removed. Saturated concentrations of ethanol in the reactor were created by injecting 0.2 mL of neat ethanol into the bottom of the reactor and allowing it to equilibrate. Reactor septa were removed for flushing the reactor with air between sample runs.

2.4. Sorption reactions/concentration recognition reactions

Initial work focused on self-recognition of surface contamination and contaminant concentration determinations. Two types of experiments were performed: those in dry zero chromatographic air (herein referred to as dry air) and those performed in humid air (40% relative humidity). In both types of reactions, the glass reactor housing all components was purged with air then was injected with the appropriate concentration of ethanol. The chemicals equilibrated for 20 minutes and the electrical resistances were recorded. The reactor was flushed with air until the sensor surface exhibited a resistance of greater than 2000 megaohms, and the next experiment commenced. The experiments were repeated using four sensors and results were averaged.

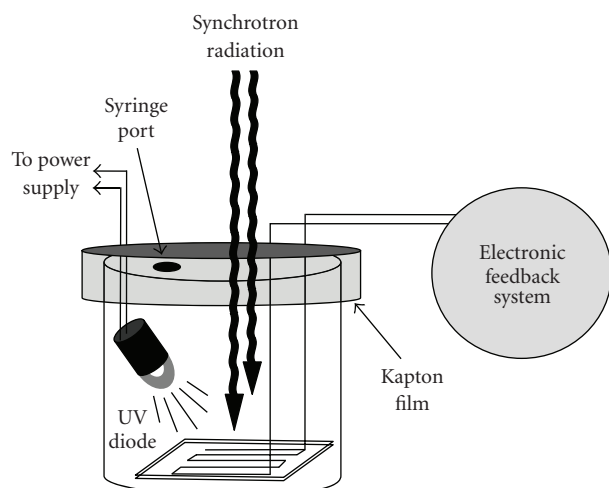


FIGURE 2: Test setup in XRF cups.

2.5. Automated detection/automated decontamination reactions

The next group of experiments focused on contaminant detection, initiation of a decontamination process, and self-monitoring of the progress of the decontamination effort. Ethanol at various concentrations was injected into the reactor in darkness, while the system continuously self-monitored film resistance. The system was programmed to switch on the UV diode should the resistance of the surface decrease by more than 10 megaohms (from a maximum detection limit of 2000 megaohms). Triggering of the UV diode also signaled the system to record the surface resistance for the next 30 minutes during illumination.

2.6. Titanium nearest neighbor/valence state monitoring

Reactions were performed in X-ray fluorescence (XRF) cups so that the bulk state of titanium could be monitored for both valence state changes and the nearest neighbor changes with X-ray absorption fine spectroscopy (XAFS). XAFS experiments were conducted at Argonne National Laboratory's Advanced Photon Source. The experiments examined the state of Ti on the prepared films in lightness and darkness in air atmospheres, in nitrogen atmospheres, and in air atmospheres saturated with ethanol.

The test configuration was essentially the same as the one used in Figure 1, only the coated substrates were contained in XRF cups sealed with Kapton film. The experimental setup is shown in Figure 2.

XAFS work was performed at Argonne National Laboratory's Advanced Photon Source, at GSECARS beamline 13BM. Samples were positioned 45° to the beam. The extended X-ray absorption fine spectroscopy (EXAFS) spectra were recorded in fluorescence mode as a function of incident X-ray energy from a water-cooled Si(111) monochromator by measuring the integrated Ti K fluorescence intensity using a 16-element Ge detector placed

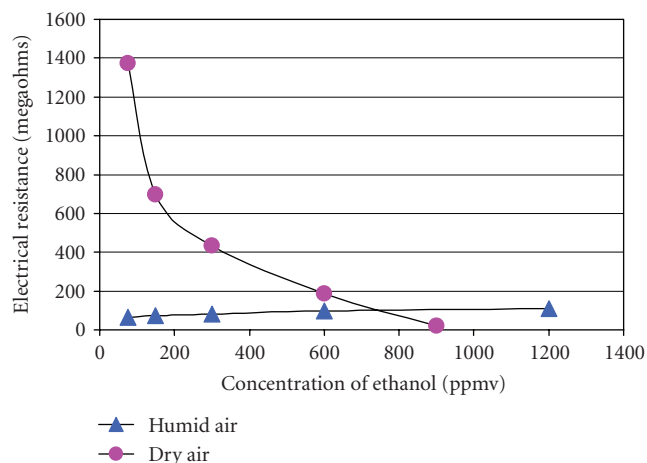


FIGURE 3: The electrical resistance of the coated substrates in dry air and in humid air in darkness as the ethanol concentration in the atmosphere above the substrates progressively increases.

in the horizontal plane along the polarization vector of the synchrotron radiation. Contaminants were injected into the XRF cup reactor and enclosed films were monitored for state changes after these injections.

3. RESULTS AND DISCUSSION

The electrical resistance of the TiO₂ surfaces changed as various concentrations of ethanol were introduced into the reactor. Figure 3 shows how the resistance of the TiO₂ film decreases as ethanol concentrations are increased in dry air and how the electrical resistance of the film slightly increases in humid air in the dark.

In dry air and in humid air, the film resistance was greater than 2000 megaohms in the absence of ethanol. In dry air in the dark, the electrical resistance rapidly decreases from 1374 megaohms at 75 ppmv ethanol to 22 megaohms at 900 ppmv ethanol. In humid air in darkness, the electrical resistance of the sensing surface slowly increases over time from 66 megaohms at 75 ppmv ethanol to 110 megaohms at 1200 ppmv ethanol. Figure 3 shows that water clearly competes for sorption sites on the TiO₂ sensing surface in darkness.

The known resistances gathered in Figure 3 were used to construct a feedback loop, whereby the sensing surface could trigger a UV LED positioned above it. Figure 4 shows how the resistance of the films in humid air (70% relative humidity) evolves as illumination proceeds.

As illumination proceeds, the resistance of the TiO₂ films decreases slightly indicating that activity is occurring on the sensing surface. Since the concentrations of injected ethanol were high and the film surface was small (1 cm by 1 cm), the oxidation of all ethanol in the reactor was not complete due to time and material constraints. However, the oxidation of gas-phase ethanol is a well-documented reaction and in the literature [13–18]. Briefly, part of the ethanol reacts on the Degussa P25 TiO₂ surface through the decomposition pathway of ethanol → acetaldehyde → acetic acid → carbon

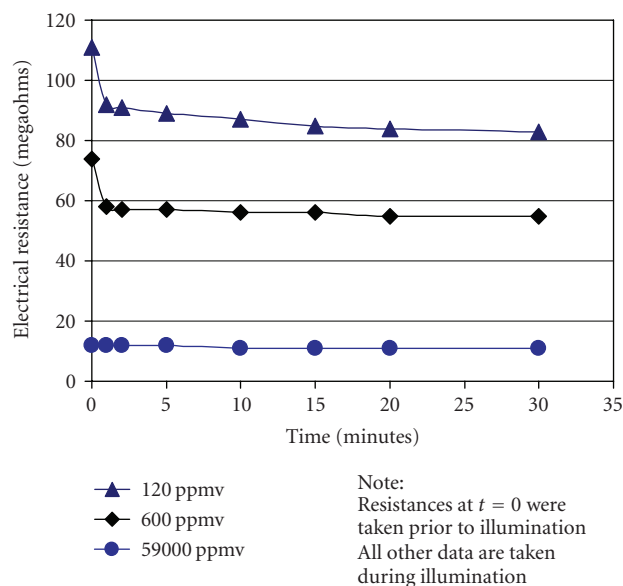


FIGURE 4: Substrate response after humid air was spiked ethanol and illuminated. Resistances at $t = 0$ reflect the surface's electrical resistance in the dark prior to the lights being turned on.

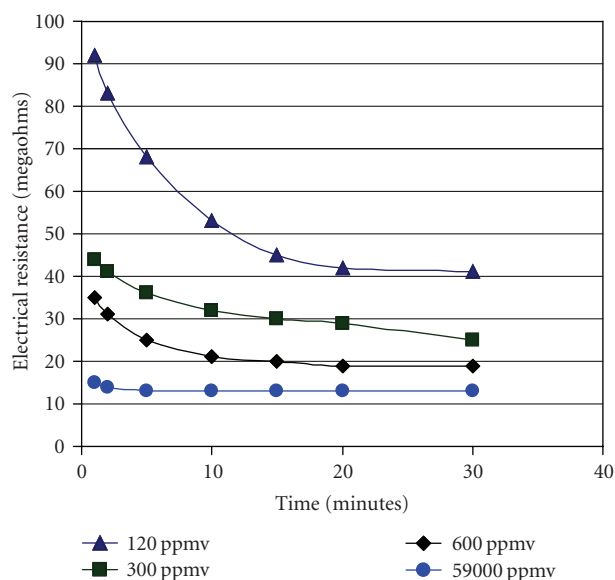
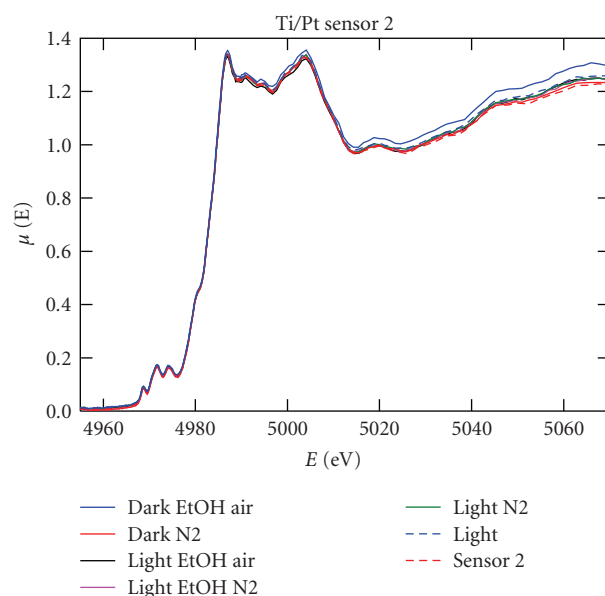


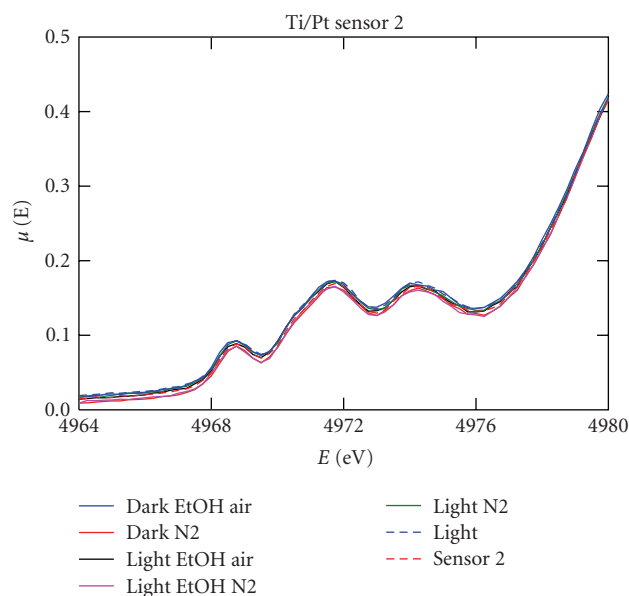
FIGURE 5: Response of substrates after dry air was spiked with ethanol and illuminated.

dioxide + formaldehyde \rightarrow formic acid \rightarrow carbon dioxide. The other portion reacts via the decomposition pathway of ethanol \rightarrow acetaldehyde \rightarrow formic acid + formaldehyde \rightarrow formic acid \rightarrow carbon dioxide [18]. Ethanol and water do compete for reaction sites on the TiO_2 surface [17], and the rate of ethanol decomposition on the TiO_2 surface is partially limited by the adsorption of intermediates on the TiO_2 [14].

Analogous to the reactions described in Figure 4, various amounts of ethanol were injected into dry air in the reactor. Figure 5 shows the resistance of the films over time in humid air (70% relative humidity) as illumination proceeds.



(a)



(b)

FIGURE 6: The XAFS spectra for the sensor. The labels designate the following atmospheric conditions during X-ray interrogation. "Dark EtOH air" indicates a saturated ethanol atmosphere in darkness; "dark N2" indicates a nitrogen atmosphere in darkness; "light EtOH air" indicates a saturated ethanol atmosphere while the sensing surface is illuminated; "light EtOH N2" indicates a nitrogen atmosphere saturated with ethanol while the sensing surface is illuminated; "light N2" indicates a nitrogen atmosphere while the sensing surface is illuminated; "light" indicates a dry air atmosphere while the sensor is illuminated; and "sensor 2" indicates a dry air atmosphere while the sensor is kept in darkness. Figure 6(b) is the magnified X-ray absorption near edge spectroscopy (XANES) portion of the spectra and describes the valence state of Ti.

From $t = 0$ minutes to $t = 30$ minutes, the resistance of the TiO_2 films drops slightly indicating that reactions are proceeding on the sensing surface. The results in both Figures 4 and 5 show that during illumination, humidity does not appear to affect the activity of surfaces exposed to saturated concentrations of ethanol; little change occurs in the resistance of the sensor over time. However, the presence of humidity does affect both the sorption of ethanol to the sensor surface (as shown in Figure 3) and the activity on the sensor surface at lower concentrations of ethanol. For example, exposure of the sensing surface to 600 ppmv of ethanol in the dark in humid air produces a resistance of 96 megaohms versus 185 megaohms in dry air. After the sensing surface is illuminated for 30 minutes, the resistance of the sensing surface in humid air decreases to 55 megaohms, while the resistance of sensing surface in dry air decreases to 19 megaohms. Humidity does play an important role in contaminant sorption to and photoactivity of Degussa P25. Muggli et al. note that water competes for sites when lights are off but at high concentrations of ethanol (100 ppm) water does not compete as effectively as ethanol [17]. Others also have noted in their oxidative work with gaseous toluene and acetone [19, 20].

Results from the XAFS studies of the bulk TiO_2 in the sensing surface are shown in Figures 6(a) and 6(b).

Figure 6 shows that in all cases, bulk Ti in the TiO_2 film remains in a Ti^{4+} state which is expected. Grazing incidence XAFS was not performed but may show variation in the state of surface Ti atoms. Films composed of smaller TiO_2 particles (i.e., nanoparticles less than 2 Å in diameter) might show variations in the state of Ti in the XANES spectra, but it is expected that the reactions with ethanol also would be different if nanoparticles were used. The spectra in Figure 6 aligns with the anatase form of TiO_2 , which is the primary form of the Degussa P25 TiO_2 used to create films.

4. CONCLUSION

This study demonstrates that films combined with an appropriate feedback system can be used to detect contaminants on their surfaces, recognize the concentration of the contaminant, and trigger a decontamination step. Humidity did affect concentration measurements of ethanol and needed to be monitored in conjunction with the resistances to produce correct concentration information in the feedback loop. XANES measurements showed that the bulk TiO_2 composing the films was in the form of anatase and the Ti remained in a 4+ valence state throughout the experiments. We expect that with advancements in nanomaterials and nanocircuits, films and materials that are self-sense and self-decontaminate will be staples of future first responders and warfighters.

ACKNOWLEDGMENTS

The authors would like to thank Dr. Andrew Mills of the University of Strathclyde for supplying the Degussa P25 TiO_2 , Mr. Joseph Gregar of Argonne National Laboratory for fabricating the quartz reactor, and Mr. Rich Voogd of

Argonne National Laboratory for fabricating the device in the reactor that connected the electronics to the sensor.

REFERENCES

- [1] T. V. Malleswara Rao and G. Deo, "Ethane and propane oxidation over supported $\text{V}_2\text{O}_5/\text{TiO}_2$ catalysts: analysis of kinetic parameters," *Industrial and Engineering Chemistry Research*, vol. 46, no. 1, pp. 70–79, 2007.
- [2] A. V. Vorontsov, D. V. Kozlov, P. G. Smirniotis, and V. N. Parmon, " TiO_2 photocatalytic oxidation: II. Gas-phase processes," *Kinetics and Catalysis*, vol. 46, no. 3, pp. 422–436, 2005.
- [3] O. d'Hennezel, P. Pichat, and D. F. Ollis, "Benzene and toluene gas-phase photocatalytic degradation over H_2O and HCL pretreated TiO_2 : by-products and mechanisms," *Journal of Photochemistry and Photobiology A*, vol. 118, no. 3, pp. 197–204, 1998.
- [4] V. Brezová, A. Blažková, L. Karpinský, et al., "Phenol decomposition using $\text{M}^{n+}/\text{TiO}_2$ photocatalysts supported by the sol-gel technique on glass fibres," *Journal of Photochemistry and Photobiology A*, vol. 109, no. 2, pp. 177–183, 1997.
- [5] A. Mills and J. Wang, "Simultaneous monitoring of the destruction of stearic acid and generation of carbon dioxide by self-cleaning semiconductor photocatalytic films," *Journal of Photochemistry and Photobiology A*, vol. 182, no. 2, pp. 181–186, 2006.
- [6] N. S. Allen, M. Edge, G. Sandoval, J. Verran, J. Stratton, and J. Maltby, "Photocatalytic coatings for environmental applications," *Photochemistry and Photobiology*, vol. 81, no. 2, pp. 279–290, 2005.
- [7] H. Z. Abdullah, H. Taib, and C. C. Sorrell, "Coating methods for self-cleaning thick films of titania," *Advances in Applied Ceramics*, vol. 106, no. 1–2, pp. 105–112, 2007.
- [8] A. Bozzi, T. Yuranova, and J. Kiwi, "Self-cleaning of wool-polyamide and polyester textiles by TiO_2 -rutile modification under daylight irradiation at ambient temperature," *Journal of Photochemistry and Photobiology A*, vol. 172, no. 1, pp. 27–34, 2005.
- [9] K. Qi, W. A. Daoud, J. H. Xin, C. L. Mak, W. Tang, and W. P. Cheung, "Self-cleaning cotton," *Journal of Materials Chemistry*, vol. 16, no. 47, pp. 4567–4574, 2006.
- [10] L. R. Skubal, N. K. Meshkov, and M. C. Vogt, "Detection and identification of gaseous organics using a TiO_2 sensor," *Journal of Photochemistry and Photobiology A*, vol. 148, no. 1–3, pp. 103–108, 2002.
- [11] L. R. Skubal, M. C. Vogt, and N. K. Meshkov, "Monitoring the electrical response of photoinduced organic oxidation on TiO_2 surfaces," in *Water, Ground, and Air Pollution Monitoring Remediation*, T. Vo-Dinh and R. L. Spellacy, Eds., vol. 4199 of *Proceedings of SPIE*, pp. 157–164, Boston, Mass, USA, November 2000.
- [12] J. F. Porter, Y.-G. Li, and C. K. Chan, "The effect of calcination on the microstructural characteristics and photoreactivity of Degussa P-25 TiO_2 ," *Journal of Materials Science*, vol. 34, no. 7, pp. 1523–1531, 1999.
- [13] N. R. Blake and G. L. Griffin, "Selectivity control during the photoassisted oxidation of 1-butanol on titanium dioxide," *Journal of Physical Chemistry*, vol. 92, no. 20, pp. 5697–5701, 1988.
- [14] M. R. Nimlos, E. J. Wolfrum, M. L. Brewer, J. A. Fennell, and G. Bintner, "Gas-phase heterogeneous photocatalytic oxidation

- of ethanol: pathways and kinetic modeling,” *Environmental Science and Technology*, vol. 30, no. 10, pp. 3102–3110, 1996.
- [15] J. M. Coronado, S. Kataoka, I. Tejedor-Tejedor, and M. A. Anderson, “Dynamic phenomena during the photocatalytic oxidation of ethanol and acetone over nanocrystalline TiO_2 : simultaneous FTIR analysis of gas and surface species,” *Journal of Catalysis*, vol. 219, no. 1, pp. 219–230, 2003.
- [16] A. V. Vorontsov and V. P. Dubovitskaya, “Selectivity of photocatalytic oxidation of gaseous ethanol over pure and modified TiO_2 ,” *Journal of Catalysis*, vol. 221, no. 1, pp. 102–109, 2004.
- [17] D. S. Muggli, K. H. Lowery, and J. L. Falconer, “Identification of adsorbed species during steady-state photocatalytic oxidation of ethanol on TiO_2 ,” *Journal of Catalysis*, vol. 180, no. 2, pp. 111–122, 1998.
- [18] D. S. Muggli, J. T. McCue, and J. L. Falconer, “Mechanism of the photocatalytic oxidation of ethanol on TiO_2 ,” *Journal of Catalysis*, vol. 173, no. 2, pp. 470–483, 1998.
- [19] Y. Ku, K.-Y. Tseng, and W.-Y. Wang, “Decomposition of gaseous acetone in an annular photoreactor coated with TiO_2 thin film,” *Water, Air, & Soil Pollution*, vol. 168, no. 1–4, pp. 313–323, 2005.
- [20] T. N. Obee, “Photooxidation of sub-parts-per-million toluene and formaldehyde levels on titania using a glass-plate reactor,” *Environmental Science & Technology*, vol. 30, no. 12, pp. 3578–3584, 1996.

